Christoph Brinkrolf[1] / Nadja A. Henke[2] / Lennart Ochel[1,3] / Boas Pucker[4,5] / Olaf Kruse[6] / Petra Lutter[7]

Modeling and Simulating the Aerobic Carbon Metabolism of a Green Microalga Using Petri Nets and New Concepts of VANESA

[1] Bielefeld University, Faculty of Technology, Bioinformatics Department, Bielefeld, Germany, E-mail: cbrinkro@cebitec.uni-bielefeld.de
[2] Bielefeld University, Faculty of Biology and CeBiTec, Genetics of Prokaryotes, Bielefeld, Germany
[3] Linköping University, Department of Computer and Information Science, Linköping, Sweden
[4] Bielefeld University, Faculty of Biology and CeBiTec, Genome Research, Bielefeld, Germany
[5] University of Cambridge, Department of PlantSciences, Evolution and Diversity, Cambridge, UK
[6] Bielefeld University, Faculty of Biology and CeBiTec, Algae Biotechnology and Bioenergy, Bielefeld, Germany
[7] Bielefeld University, Faculty of Biology and CeBiTec, Proteome and Metabolome Research, Bielefeld, Germany

Abstract:
In this work we present new concepts of VANESA, a tool for modeling and simulation in systems biology. We provide a convenient way to handle mathematical expressions and take physical units into account. Simulation and result management has been improved, and syntax and consistency checks, based on physical units, reduce modeling errors. As a proof of concept, essential components of the aerobic carbon metabolism of the green microalga *Chlamydomonas reinhardtii* are modeled and simulated. The modeling process is based on xHPN Petri net formalism and simulation is performed with OpenModelica, a powerful environment and compiler for Modelica. VANESA, as well as OpenModelica, is open source, free-of-charge for non-commercial use, and is available at: http://agbi.techfak.uni-bielefeld.de/vanesa.

Keywords: *Chlamydomonas reinhardtii* , metabolic network, OpenModelica, systems biology, xHPN
DOI: 10.1515/jib-2018-0018
Received: March 2, 2018; **Revised:** August 5, 2018; **Accepted:** August 16, 2018

1 Introduction

Modeling biological systems is necessary to understand and predict behavior. Depending on available information about the system of interest, different modeling approaches can be selected, e.g. static versus dynamic, discrete versus continuous or deterministic versus probabilistic. There is a choice between rule-based systems, grammars and corresponding automata, or graph-based approaches such as Petri nets. This paper focuses on Petri net-based modeling and simulation. A basic knowledge of Petri nets is assumed. For an introduction to Petri nets, readers should consult [1]. The definition of hybrid Petri nets (HPN) is given in [2], and the extension of HPN to hybrid functional Petri nets (HFPN) is nicely described in [3].

One advantage of HPN is the flexibility of modeling. Even if very little information is available, a discrete Petri net approach can be applied. With advances in high throughput measurement techniques in systems biology, an increasing amount of large-scale biological data will be produced. These quantitative data sets enable the construction of (partially) quantitative models which can be realized using HFPN formalism.

Accurate modeling and simulation requires an appropriate formalism as well as efficient and accessible software. There are only few tools available which allow modeling and simulation of HFPN, such as Cell Illustrator [4] and Snoopy [5]. Cell Illustrator is a commercial tool with a graphical user interface (GUI) is designed for systems biology applications. The Petri net framework Snoopy offers various Petri net classes for modeling and simulation. The extended hybrid Petri net formalism (xHPN) [6] unifies different Petri net concepts, such as HPN, HFPN, and stochastic Petri nets [7], among others. It offers hybrid modeling using discrete, continuous, and stochastic transitions as well as discrete and continuous places and standard arcs, inhibitory arcs, and test arcs. Functions, depending not only on current marking of the Petri net, can be attached to any arc and to continuous transitions as speed function. Activation of transitions can be manipulated by boolean expressions.

Christoph Brinkrolf is the corresponding author.

Places may have upper and lower capacities. Furthermore, strategies for Petri net conflict solution can be set. A description of all available elements and attributes is given in [6], a brief mathematical definition is given in [8], and the extensive definition is given in [9]. xHPN has already been deployed in biological as well as in non-biological application cases. The open source library PNlib [6] implements the xHPN formalism and is written in the equation-based object-oriented modeling language Modelica [10]. Due to the complete specification of conflict handling within the formalism (and thus within the library), the library is independent of the software which is used for compilation and simulation. It leads to transparent and comparable simulation results, which is not the case for black box implementations. Free and commercial Modelica compilers are available, e.g. OpenModelica, JModelica, and Dymola [11].

VANESA [12] is a software for modeling, simulating and analyzing biological networks. A typical workflow is shown in Figure 1. The process of modeling can either be supported by data stored in the data warehouse or by creating a network manually, based on lab and/or literature data. The data warehouse DAWIS-M.D. [13] integrates several molecular biological databases, such as KEGG [14], Brenda [15] and PPI databases (IntAct [16], MINT [17], HPRD [18]). VANESA accesses the data warehouse via web service. The resulting network can be edited and further transformed into a Petri net. This transformation is necessary for simulation. Simulation is performed by the OpenModelica compiler (OMC) [19]. Petri nets are exported as Modelica models and are compiled with the Petri net library PNlib. Exporting the Modelica model and calling the OMC is done by VANESA in the background. The user only needs to interact with VANESA. After the simulation process is finished, simulation results are visualized in VANESA and can be examined. With these insights the model can be adjusted, which leads to a new run of the workflow. Additionally, biological networks as well as Petri nets can be analyzed by implemented graph algorithms.

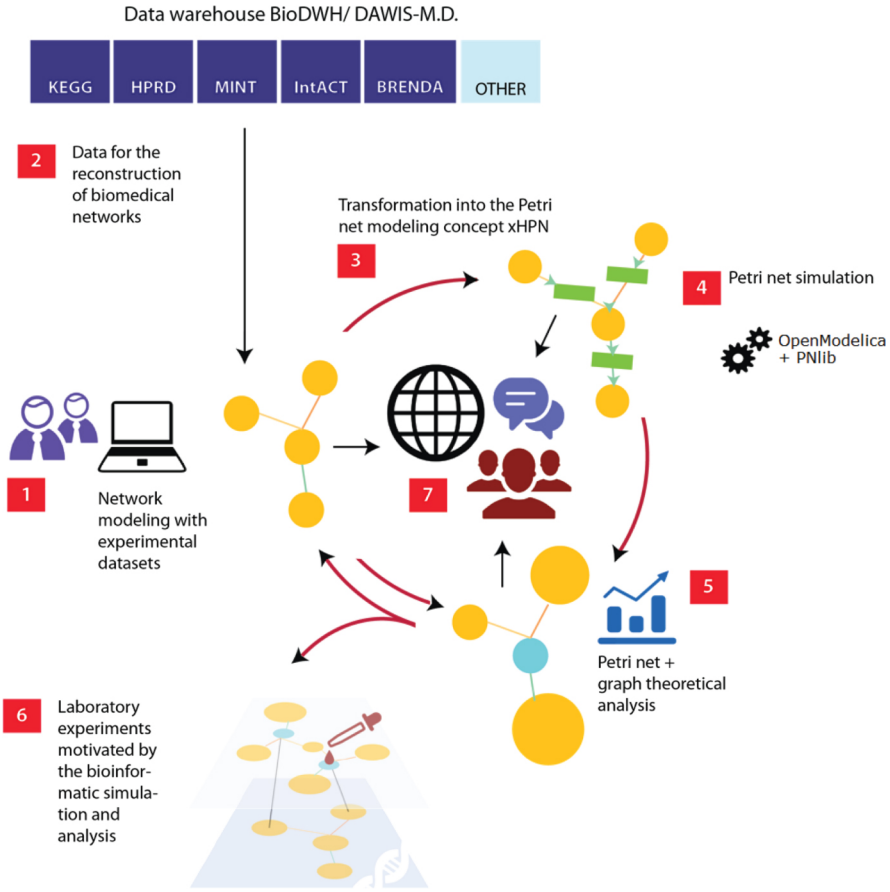

Figure 1: Workflow of VANESA: (1) create biological network using prior knowledge, (2) use the data warehouse, (3) transform biological network into Petri net, (4) perform Petri net simulation, (5) analyze Petri net and biological network, (6) insights could lead to new experiments and (7) share network with others [12].

VANESA has already been applied in several case studies [12]. Facing the immense complexity of biological networks, detailed modeling often requires dealing with the integration of complex functions as they occur, e.g. in kinetics. This leads to the following new requirements:

- Support of kinetic equations including physical units
- New connection to simulation executable

- Support of entire xHPN formalism
- Advanced visualizations (simulation results, logical nodes)

VANESA allows modeling of sophisticated biological systems such as metabolism, which is influenced by many factors such as enzyme concentration and activity, concentration of metabolites and co-factors, inhibitory and amplifying effects. Knowledge of the impact of these factors and the dynamics of their kinetic interplay is essential for a complete understanding of the system.

The green alga *C. reinhardtii* is one model organism which produces hydrogen under certain stress conditions [20]. Since improving hydrogen production is of enormous economic interest, an enhanced understanding of the system through modeling would facilitate commercial developments. One of the best ways to describe the behavior of a biological system in a large-scale industrial set-up is a deterministic model [21].

Predicting the evolution of the key factors of the metabolic system under consideration is of high interest due to an increasing amount of biotechnological production processes, e.g. biofuel [22], [23], hydrogen production [24], and amino acids [25].

The new features required to model such systems were analyzed, and the implementation of appropriate new concepts and features extends VANESA significantly. The current release of VANESA (0.3.2) containing the concepts and features is available from http://agbi.techfak.uni-bielefeld.de/vanesa. In order to demonstrate the functionality of our novel model platform, we chose a metabolic network mapping relevant aspects of the carbon metabolism of the green microalga *C. reinhardtii* under aerobic growth conditions. This network comprises, inter alia, the gluconeogenesis.

2 Architecture/Implementation/Workflow

In the following, we describe important changes of VANESA, and compare them with the implementations of Cell Illustrator 4.0 (latest scientific publication) and Snoopy 1.21.

2.1 Mathematical Expressions and Physical Units

Extraction of parameters

The rate of change of metabolite concentrations is given by the kinetics of enzymes. The mathematical functions describing kinetics may have a simple or a rather complex structure with several parameters. Parameters, such as k_m (Michaelis-Menten constant) values, may occur multiple times in one kinetic function, making the separation of parameter values and the mathematical function including these parameters desirable. In this manner the value of a parameter can be easily updated without changing the structure.

Syntax check and rendering

A kinetic function may consist of several fractions composed of nested terms which are usually grouped by brackets. This structure is distinct but may be non-intuitive for complex functions. Manually editing functions may introduce human error. Thus, we implemented an approach which parses functions and determines if they represent a valid mathematical function. If a mistake is detected, the position in the function is output, while if they are correctly parsed they are rendered easily recognizable in LaTeX.

Physical units

Each parameter has three attributes: name, value, and physical unit. For the process of modeling, units may remain unspecified. Units are taken into account before a simulation is performed. The OMC analyzes all mathematical expressions and parameters. For parameters and expressions which have not been assigned a unit, the appropriate unit is computed. If no unit can be assigned, feedback is given to the user. Additionally, it is verified that the unit of speed functions describes a change over time e.g. $\frac{\text{mol}}{\text{s}}$. Performing this analysis has two advantages, namely that wrong units can be detected very fast and that structural verification of expressions can reveal hidden mistakes. For example, the expression $(a - b)/c$ may be mistakenly given as $(a - b/c)$. The syntax of both expressions is valid, so the mistake cannot be revealed by the syntax check itself. If units are taken into account, a and b have to have the same unit and if unit of $a \neq$ unit of $\frac{b}{c}$ the mistake can be detected.

2.2 Further Modeling Features

Knock out of reactions

Knocking out a reaction is a common way to investigate the influence of this specific reaction on the modeled system. If a reaction is knocked out, it neither consumes nor produces any substances, which is equal to a maximum reaction rate of 0. For the simulation process of a Petri net, the maximum speed function of each knocked out transition is thus exported as 0. Alternatively, all connected arcs of a knocked out transition could be deleted, but this would change the topology of the Petri net.

Constant metabolites

In complex biological systems the concentration of almost every metabolite depends on reactions and in turn influences the reaction rates. In an early stage of modeling or for a thorough investigation of a system, it might be helpful to neglect the concentration dynamics of a particular metabolite, but not the numerical concentration value. In a Petri net a constant metabolite is represented by a place, where the weight of its incoming arcs is set to 0 and its outgoing standard arcs are replaced by test arcs.

Logical elements

In Petri nets, each place (or represented metabolite) may occur only once. Metabolites (such as ATP, ADP) which are involved in several reactions are represented by a single place. While in network visualization, one such place may occur multiple times in different positions as a visual aid, only one copy is present in the exported Petri net.

Support of entire xHPN formalism

In this version, the entire xHPN formalism is available for modeling. Support of speed functions for continuous transitions, conditions, and conflict solving strategies are among the important additional concepts that were added. Speed functions are beneficial for modeling kinetics. The reaction speed is represented by the maximum speed of the continuous transition. A continuous transition, in general, does not have a speed function as an attribute. Thus, the speed function was multiplied with the arc weight of each connecting arc.

2.3 Simulation and Visualization

The simulation of a Petri net is performed by employing OMC of OpenModelica release 1.12.0. The Petri net is exported as Modelica code, which is compiled together with the PNlib by OMC. The major change is the execution of the compiled simulation. In the past, the compiled simulation was executed and afterward, the file containing the simulation results was loaded and visualized. The major changes are described in the following.

Connection to OMC

Besides the compilation of the Petri net model, advanced features of OMC are used. One of these features is the unit check. Additionally, OMC performs further analysis and consistency checks of the model. All warnings and errors are then reported to the user.

The communication of VANESA and the simulation executable is realized by the TCP/IP Client-server model. VANESA is the server and waits for the connection of the simulation client. When the connection is established, the simulation result for each computed time step is sent as byte stream and processed. If problems occur while execution (such as numerical problems of the integrator), warnings and errors are shown to the user. Based on the simulation result and the feedback the user can stop the execution of the simulation and can adjust the model. It is not necessary to wait until the execution has finished.

Visualization of simulation results

Simulation results are dynamically visualized while the simulation is running. In contrast to previous releases, the user does not have to wait until the simulation process has finished. As for places, the chart shows the number of tokens for each time step, and for the transitions, the actual firing speed for each time step is shown. For arcs two functions are drawn, the actual token flow and the cumulated token flow. If multiple places are selected, the chart shows the number of tokens for the selected places. If only one node or arc is selected, the chart shows all stored simulation results of this entity.

The distribution of tokens for a particular time step can be shown by the use of the slider. If the slider is set to a specific time step, the number of tokens for this time step is drawn in each place. Transitions which are active at this time step are colored red.

If one simulation result is selected, the detailed view shows the tokens of all places for all time steps in a table and plots a chart for the tokens of each place. These charts are either scaled individually or have the same scaling. Individual scales focus on the individual properties of each place. Enabling a common scaling for all charts makes it possible to focus on the global behavior of change of tokens.

2.4 Exports and Documentation

Graphics and simulation results

The graph displaying the modeled system as well as charts showing simulation results, can be exported in various formats, such as PNG, SVG and PDF. Excerpts can also be created by zooming in on the desired area. A single simulation result can be exported in CSV format to analyze raw simulation data with external tools and to share the data. This export includes all attributes that are visualized in graphs (places, transitions and arcs). Additionally, this file can be also imported and mapped to the graph as a simulation result.

LaTeX export

Sharing a whole model is important for collaborative work and for the transparency. For this purpose, we implemented LaTeX export of models. This export generates a LaTeX file, which can be compiled as a PDF. It contains an image of the graph (as it is visualized in VANESA), all initial values, all equations showing preconditions, postconditions, speed functions, and all parameters of each equation. If the model takes units into account, the unit is exported for all initial values and parameters as well. In the table of initial values it is also indicated whether a place has a constant amount of tokens. If equations are disabled (in biology: "knocked-out"), it is also shown that their speed function equals 0. This automatically-generated document provides all information necessary to model or adapt the system.

SBML L3v1 export

The default format for storing and loading models of VANESA is Systems Biology Markup Language (SBML). Attributes of the model which are not supported by SBML natively are stored as *SBML annotations*. The model is stored independently of possible simulation results because simulation results would increase the size of the SBML file drastically, and further processing of simulation results with external tools will be easier using the more general CSV format. The export was updated to Level 3 version 1 [26]. Using JSBML library ensures that the saved model is a valid SBML model.

2.5 Comparison and Discussion of Features

An overview of the new features of VANESA in comparison to already implemented features of Cell Illustrator and Snoopy is provided in Table 1. Some of the features, such as (image) export of simulation results are implemented in Cell Illustrator and Snoopy, while some features are implemented in only one of the tools. Snoopy has a strong support of mathematical expressions and only lacks rendering of expression while modeling. In VANESA a LaTeX rendering of mathematical expressions is provided as export. Concepts of constant places and knocked out transitions are implemented in a very user friendly way as check boxes. In Snoopy constant places are also realized as check boxes and speed functions of transition are assigned to different *function sets*. For the simulation one function set has to be chosen. Cell Illustrator does not have a native support for the concept of constant places and knocked out transitions.

Table 1: Comparison of new features of VANESA with Cell Illustrator and Snoopy.

VANESA feature	Cell Illustrator	Snoopy
Extraction of variables	no	yes
Syntax check	yes	yes
Rendering of expressions	no	no
Physical units	yes	no
Knock out	(yes)	yes
Constant metabolites	no	yes
Capacities	yes	no
Logical elements	no	yes
HFPN support	yes	(yes)
Definition of conflict handling	yes	no
Visualization of sim. res. for places, transitions, arcs	yes, yes, no	yes, yes, no
Image export	yes	yes
LaTeX export	no	yes

The major difference of VANESA and Snoopy is the Petri net formalism. Speed functions of transitions may only depend on constants and pre-places, but not on other places of the Petri net [26]. In Snoopy, the use of *modifier arcs* is mandatory to define reaction speeds which depend on other places than those representing substrates, but modifier arcs do not affect the network topology and the Petri net semantics. In contrast to Cell Illustrator, Snoopy does not provide enabling conditions, the concept of lower and upper capacities, and the definition of conflict handling (e.g. set priorities of transitions). A unique feature of VANESA is the visualization of the token flow of arcs.

In general, the use of bio-semantics in Snoopy allows for the coincidence of non-enabledness and zero speed functions yielding non-negative markings, which is accepted to permit significant performance enhancement but might not be desirable by the user. The recently published adaptive semantic [27] which ensures non-negative marking of pre-places is implemented in Snoopy for continuous Petri nets, but it does not apply for continuous parts of a hybrid Petri net. Thus, in continuous parts of a hybrid network, the number of tokens may get negative. In addition, if the speed function of a continuous transition in a continuous or hybrid Petri net becomes negative, the flow of tokens becomes reversed (from post-places to pre-places). This makes it very difficult to comprehend and compare the simulation results of Snoopy. The implementation of PNlib ensures the non-negativity of markings and speed functions.

3 Application

3.1 Characteristics of the Carbon Metabolism of *C. Reinhardtii*

The carbon metabolism of *C. reinhardtii* consists of many pathways, e.g. glycolysis, gluconeogenesis, citric acid cycle, fermentative pathways, etc. The modeler has to make a choice as to what extent different pathways are represented in the model. For our application case we want to demonstrate how metabolic pathways relevant for the algal behavior under aerobic conditions are transferred into a mathematical model.

Besides photoautotrophic growth using carbon dioxide and light energy for assimilation processes [28], this green freshwater alga can also consume acetate as a carbon and energy source to build up biomass under aerobic conditions (heterotrophic growth) [29].

The generation of sugars from non-sugar carbon sources proceeds via gluconeogenesis, which is the reverse pathway of glycolysis. In order to ensure metabolic flow in the direction of glucose production (Glc), some antagonistic reactions are catalyzed by dedicated enzymes. This enables a precise regulation depending on the metabolic situation in a cell. First, acetate is taken up and converted into acetyl coenzyme A (Acetyl-CoA). Acetyl-CoA feeds the tricarboxylic acid (TCA) cycle, and in the following oxaloacetate (OAA) is converted into phosphoenolpyruvate (PEP). PEP is then used for the synthesis of longer carbon chain compounds. An overview is displayed in Figure 2.

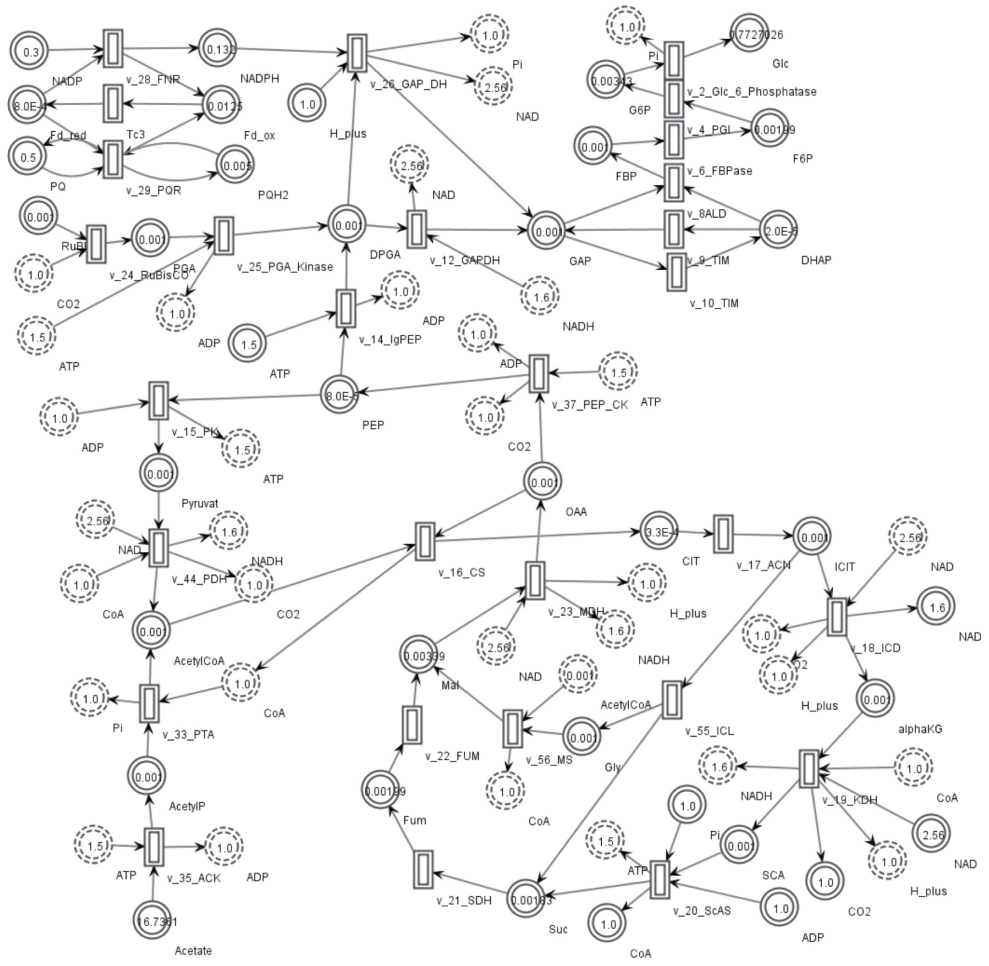

Figure 2: Petri net of the aerobic model. Places with dashed border represent logical elements.

3.2 Data Sources and Challenges

Literature and databases represent important information sources if novel generated data is not available. We made use of BRENDA [15] and a specific set of publications for the missing kinetic values describing reaction velocities v_i: v_{33}, v_{35}, v_{44} [30], v_4, v_6, v_8, v_9, v_{10}, v_{12}, v_{14}, v_{15} [31], v_{37} [32], v_{28}, v_{29} [33], v_2 [34], v_{16}, v_{17}, v_{18}, v_{19}, v_{20}, v_{21}, v_{22}, v_{23}, v_{55}, v_{56} [35], and v_{24}, v_{25}, v_{26} [36]. In the best case, the publication provides the kinetics (speed function) with all its parameters for the desired enzyme. If a reaction is to be reversed, the kinetics can be transformed to provide the desired direction. If only parameters are available, a suitable kinetic law (such as reversible/irreversible Michaelis-Menten) has to be chosen and applied. Time in the model is given in minutes.

Evidently, knowledge of the parameters as k_m and k_{cat} (turn-over rate) values is essential. Some of the used k_m and k_{cat} values were retrieved from selected publications and complemented with information from BRENDA. Some parameters were set according to information about other species due to limited information about the corresponding enzymes of *C. reinhardtii*.

The entire set of these ordinary differential equations, parameters, and initial values can be found in the generated documentation in supplement.

Apart from speed functions and their parameters, initial concentrations for metabolites are essential for the model. Integration of these values into the model offers the user the opportunity to adjust the model to desired requirements, even if data on enzymes is solely taken from databases. In our example, all initial values are set according to own lab data, wherever possible. Model compartments are omitted. This results in exactly one initial concentration for each metabolite. Moreover, some metabolites held constant.

3.2.1 Estimation of Physiological Concentrations

Precise quantification of metabolic concentrations is often critical to achieve. As a consequence, there are only values for a few organisms available. Cellular concentrations of highly instable substances like NADH or ATP

are rarely quantified. Therefore, we collected values from a huge variety of different species and looked at the ranges and the distribution of physiological concentrations. To avoid the influence of extremophilic species on the finally selected value, we calculated the median of each data set (n representing the number of data points). This method was applied to NADPH ($n = 4$), $NADP^+$ ($n = 34$), NADH ($n = 10$), NAD^+ ($n = 40$) and ATP ($n = 11$) (Supplementary Table 1). Due to a paucity of known intracellular concentrations, we extracted values of some substances from a single reference: O_2 [37], reduced ferredoxin [38] and oxidized ferredoxin [38].

3.3 Model Construction with VANESA

VANESA and its new features were used to construct the model. First, the topology of the aerobic system was established by creating nodes for each reaction and metabolite and connecting the nodes with respect to the reactions. Metabolites that are involved in multiple reactions are modeled as references and occur many times. In the second step, speed functions and parameters were set. Syntax checks and rendering of these functions were applied to avoid modeling errors. In the end, initial concentrations were set to the metabolites. For the process of simulation, the created biological network was transferred into a continuous functional Petri net. Each reaction is represented by a continuous transition and each place describes the properties of a metabolite. Finally, the information on physical units was used to check the mathematical expressions of the Petri net with the help of OpenModelica.

3.4 Simulation Results

The newly implemented connection between VANESA and OpenModelica as well as the visualization of simulation results were applied. The model was simulated for 20 time units of the model (in this case, time is modeled in minutes), to reach a quasi-steady-state condition for the inner metabolites. The whole process of simulation took 172 seconds (32 s for compilation and 140 s for simulation) on a i7 desktop computer with 16GB RAM. The number of evaluated intervals was set to 1000 to calculate smooth and accurate results. Selected simulation results are shown in the following. Figure 3(A) shows the temporal development of the concentration of acetate, which is one of the main substrates of the model. It is consumed by reaction v_{35}. The reaction speed of v_{35} over time is shown in Figure 3(B). It is closely related to the amount of metabolites which is consumed. The simulation results for the arc from acetate to reaction v_{35} are shown in Figure 3(C). The dashed line shows the momentary metabolite flow over time and the regular line shows the sum of metabolites until a certain time point. Obviously, the speed of v_{35} and the metabolite flow of Figure 3(C) are congruent. The simulation result of an intermediate metabolite, PEP, is shown in Figure 3(D). The initial amount gets consumed quickly, but then PEP accumulates until time point 6. The product of this model is glucose and its precursor G6P. G6P accumulates over time as shown in Figure 3(B), as well as glucose, shown in Figure 4(A). Although G6P is the precursor of glucose, it accumulates, because it is produced at a higher rate than it is consumed. It is important to have a close look at the scaling of the ordinates.

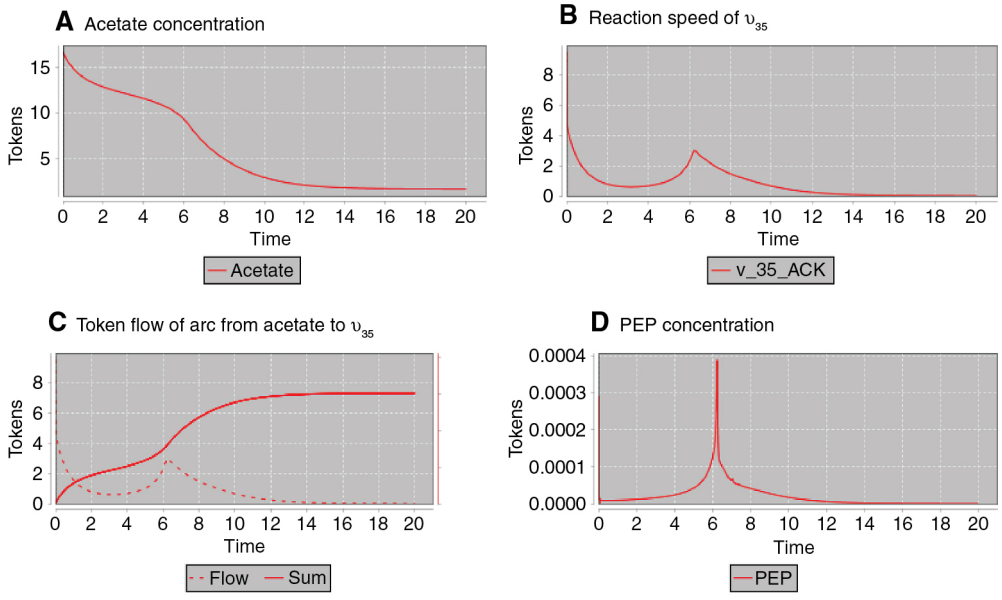

Figure 3: Simulation results of acetate, v_{35}, the arc connecting acetate and v_{35}, and PEP.

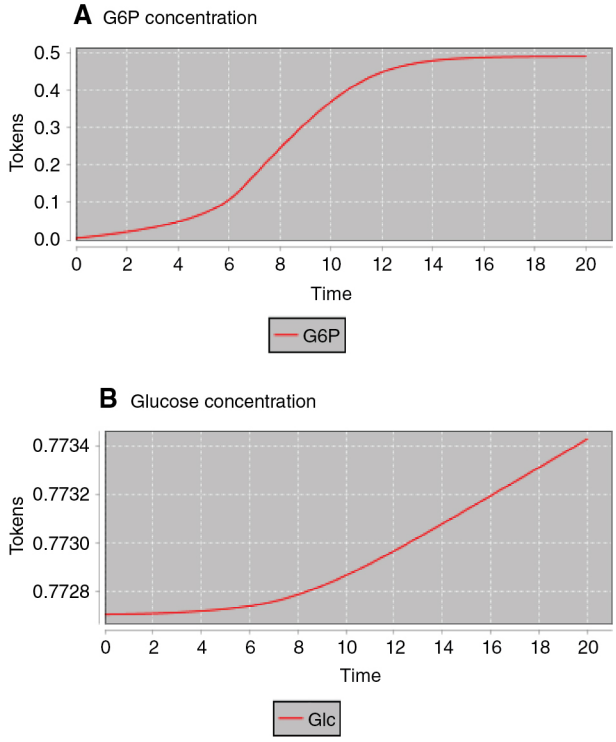

Figure 4: Simulation results of G6P and glucose.

4 Discussion and Conclusion

The new features implemented in VANESA significantly facilitated modeling the aerobic metabolism of *C. reinhardtii*. As the use of parameters and mathematical expressions from literature has been shown to be error-prone; syntax checks, consistency checks based on physical units, and the rendering of mathematical expressions are proven to be useful in avoiding mistakes. By this means, an executable model could be built and simulated easily. As the simulation results show, the dynamics are visible and the visible presentation of simulation results for each node and arc in the model helps to investigate and understand the biological process.

Due to assumptions inherent in certain kinetic laws, e.g. the concentration of the product being zero at the beginning, the simulation time in the model comprises additional time for processes that do not have to be considered in the living cell. There is, e.g. a prolonged transient response to be observed in the computer model. The time frame of the computer model could be calibrated, of course, but as comparative lab data is rather static in general (e.g. gas chromatography – "mass spectrometry measurements), it makes more sense to compare model and lab data, once a quasi-steady-state is reached. While precise quantitative lab data is not available at the moment, it can be checked, at least, whether the formation of G6P seems to be reasonable. In vivo data in *E. coli* indicate a distinct concentration of hexose-phosphates, estimated at around 8.8 mM [39]. This concentration appears to be comparable for growth on different carbon sources indicating that the pool of phosphorylated sugars remains more or less constant under different conditions and might also hold true for different organisms. In order to achieve more precise model validations flux measurements where the microalga is fed with labeled acetate could give more details on the aerobic carbon metabolism [40], [41]. Time course experiments might enable to observe relative changes in metabolite concentrations allowing a direct comparison to the simulation results. Thus, with the here mentioned simulation platform new insights of the metabolism of *C. reinhardtii* are possible. In the future, application of findings for useful purposes such as metabolic engineering approaches for e.g. established productions in the unicellular microalga such as hydrogen or terpene [42], [43], [44] are aimed at. However, this approach is easily transferable to other biological systems of industrial interest. Simulations of metabolic networks can support the identification of bottle-necks and metabolic burdens in order to increase e.g. biofuel productions.

This first model has some constraints, such as omitting compartments and neglecting temperature effects in lab data. Moreover, parameters from different species had to be included. Our approach, using extended hybrid Petri nets, makes it easy to extend and refine this model. It is also possible to include data from proteome and transcriptome as well.

The Petri net shows the dependencies and directions of metabolites and reactions, and the user is assisted with complex mathematical expressions and parameters, as they occur in kinetics. Thereby, mistakes are avoided. This shows that the combination of VANESA, xHPN formalism implemented in PNlib, and OpenModelica with all their features provides a powerful modeling and simulation environment to apply extended hybrid Petri nets in systems biology.

Acknowledgement

We are grateful to Karsten Niehaus for his support. We thank Inga Freudenau, Melanie Gerken, and Charlotte Lässig for valuable input on metabolic pathways. We thank Hanna Schilbert for her literature search to achieve values for highly instable substances. We thank Anja Döbbe for information on algal metabolism and providing values for initial metabolic concentrations. We thank Nathanael Walker-Hale for proofreading.

Funding

This work is supported by the Ministry of Innovation, Science and Research of the German State of North Rhine-Westphalia (MIWF NRW) as part of the research cooperation "MoRitS – Model-based Realization of intelligent Systems in Nano-and Biotechnologies" (grant no. 321 - 8.03.04.03 - 2012/02).

Conflict of Interest Statement: Authors state no conflict of interest. All authors have read the journal's Publication ethics and publication malpractice statement available at the journal's website and hereby confirm that they comply with all its parts applicable to the present scientific work.

References

[1] Reisig W. Petri nets: an introduction. Vol. 4 of EATCS Monographs on Theoretical Computer Science. Germany: Springer-Verlag Berlin Heidelberg; 1985.
[2] David R, Alla H. Discrete, Continuous, and hybrid petri nets, 2nd ed. Germany: Springer-Verlag Berlin Heidelberg; 2010.
[3] Matsuno H, Tanaka Y, Aoshima H, Doi A, Matsui M, Miyano S. Biopathways representation and simulation on hybrid functional Petri net. In Silico Biology. 2003;3:389–404.
[4] Nagasaki M, Saito A, Jeong E, Li C, Kojima K, Ikeda E, et al. Cell Illustrator 4.0: a computational platform for systems biology. In Silico Biology. 2010;10:5–26.
[5] Heiner M, Herajy M, Liu F, Rohr C, Schwarick M. Snoopy – a unifying petri net tool. In: Haddad S, Pomello L, editors. Application and Theory of Petri Nets. Berlin, Heidelberg: Springer Berlin Heidelberg; 2012. p. 398–407.
[6] Proß S, Bachmann B. PNlib – an advanced Petri net library for hybrid process modeling. In: Otter M, Zimmer D, editors. Proceedings of the 9th International Modelica Conference. : Linköping University Electronic Press; 2012. p. 47–56.
[7] Goss PJE, Peccoud J. Quantitative modeling of stochastic systems in molecular biology by using stochastic Petri nets. Proc Natl Acad Sci U S A. 1998;95:6750–5.
[8] Proß S, Janowski SJ, Bachmann B, Kaltschmidt C, Kaltschmidt B. PNlib – A modelica library for simulation of biological systems based on extended hybrid petri nets. In: Heiner Monika, Hofestädt Ralf, editor(s). Proceedings of the 3rd International Workshop on Biological Processes & Petri Nets (BioPPN 2012), satellite event of Petri Nets 2012, Hamburg, Germany, June 25, 2012CEUR Workshop, Proceedings Vol. 852. Hamburg, Germany: CEUR-WS.org, 2012:47–61.
[9] Proß S. Hybrid modeling and optimization of biological processes. Germany: Bielefeld University; 2013.
[10] Modelica Association. Modelica webpage. Available from: https://www.modelica.org/. Accessed on 28 August, 2018.
[11] . Modelica Association. Modelica Tools webpage Available from: https://www.modelica.org/tools/. Accessed on 28 August, 2018.
[12] Brinkrolf C, Janowski SJ, Kormeier B, Lewinski M, Hippe K, Borck D, et al. VANESA – a software application for the visualization and analysis of networks in system biology applications. J Integr Bioinform. 2014;11:239.
[13] Hippe K, Kormeier B, Töpel T, Janowski S, Hofestädt R. DAWIS-M.D. – a data warehouse system for metabolic data. In: Fähnrich KP, Franczyk B, editors. Informatik 2010: Service Science – Neue Perspektiven für die Informatik, Beiträge der 40. Jahrestagung der Gesellschaft für Informatik e.V. (GI), Band 2, 27.09. – 1.10.2010, Leipzig, Deutschland. Vol. 175 of LNI. GI; 2010. p. 720–5.
[14] Kanehisa M, Goto S, Sato Y, Furumichi M, Tanabe M. KEGG for integration and interpretation of large-scale molecular data sets. Nucleic Acids Res. 2012;40:109–14.
[15] Scheer M, Grote A, Chang A, Schomburg I, Munaretto C, Rother M, et al. BRENDA, the enzyme information system in 2011. Nucleic Acids Res. 2011;39:670–6.
[16] Kerrien S, Aranda B, Breuza L, Bridge A, Broackes-Carter F, Chen C, et al. The IntAct molecular interaction database in 2012. Nucleic Acids Res. 2012;40:841–6.

[17] Licata L, Briganti L, Peluso D, Perfetto L, Iannuccelli M, Galeota E, et al. MINT, the molecular interaction database: 2012 update. Nucleic Acids Res. 2012;40:857–61.
[18] Keshava Prasad TS, Goel R, Kandasamy K, Keerthikumar S, Kumar S, Mathivanan S, et al. Human protein reference database – 2009 update. Nucleic Acids Res. 2009;37:767–72.
[19] Fritzson P, Aronsson P, Lundvall H, Nyström K, Pop A, Saldamli L. The openmodelica modeling, simulation, and software development environment. Simulation News Europe. 2005;44:8–16.
[20] Melis A, Zhang L, Forestier M, Ghirardi ML, Seibert M. Sustained photobiological hydrogen gas production upon reversible inactivation of oxygen evolution in the green AlgaChlamydomonas reinhardtii. Plant Physiol. 2000;122:127–36.
[21] Almquist J, Cvijovic M, Hatzimanikatis V, Nielsen J, Jirstrand M. Kinetic models in industrial biotechnology â€ Improving cell factory performance. Metab Eng. 2014;24:38–60.
[22] Nozzi NE, Desai SH, Case AE, Atsumi S. Metabolic engineering for higher alcohol production. Metab Eng. 2014;25:174–82.
[23] Oliver NJ, Rabinovitch-Deere CA, Carroll AL, Nozzi NE, Case AE, Atsumi S. Cyanobacterial metabolic engineering for biofuel and chemical production. Curr Opin Chem Biol. 2016;35:43–50. Energy Mechanistic Biology.
[24] Kruse O, Rupprecht J, Bader KP, Thomas-Hall S, Schenk PM, Finazzi G, et al. Improved photobiological H2 production in engineered green algal cells. J Biol Chem. 2005;280:34170–7.
[25] Wendisch VF, Jorge JMP, Pérez-García F, Sgobba E. Updates on industrial production of amino acids using Corynebacterium glutamicum. World J Microbiol Biotechnol. 2016;32:105.
[26] Herajy M, Heiner M. Hybrid representation and simulation of stiff biochemical networks. Nonlinear Anal-Hybri. 2012;6:942–59.
[27] Herajy M, Heiner M. Adaptive and bio-semantics of continuous petri nets: choosing the appropriate interpretation. Fundam Inform. 2018;160:53–80.
[28] Johnson X, Alric J. Central carbon metabolism and electron transport in Chlamydomonas reinhardtii: metabolic constraints for carbon partitioning between oil and starch. Eukaryotic Cell. 2013;12:776–93.
[29] Chen F, Johns MR. Heterotrophic growth of Chlamydomonas reinhardtii on acetate in chemostat culture. Process Biochemistry. 1996;31:601–4.
[30] Hoefnagel MH, Starrenburg MJ, Martens DE, Hugenholtz J, Kleerebezem M, Van Swam II, et al. Metabolic engineering of lactic acid bacteria, the combined approach: kinetic modelling, metabolic control and experimental analysis. Microbiology (Reading, England). 2002;148:1003–13.
[31] Hynne F, Danø S, Sørensen PG. Full-scale model of glycolysis in Saccharomyces cerevisiae. Biophys Chem. 2001;94:121–63.
[32] Jabalquinto AM, Cardemil E. The kinetic mechanism of yeast phosphoenolpyruvate carboxykinase. Biochim Biophys Acta. 1993;1161:85–90.
[33] Laisk A, Walker DA. A mathematical model of electron transport. Thermodynamic necessity for photosystem II regulation: 'light stomata'. Proc R Soc Lond B Biol Sci. 1989;237:417–44.
[34] Reczek PR, Villee CA. A purification of microsomal glucose-6-phosphatase from human tissue. Biochem Biophys Res Commun. 1982;107:1158–65.
[35] Singh VK, Ghosh I. Kinetic modeling of tricarboxylic acid cycle and glyoxylate bypass in Mycobacterium tuberculosis, and its application to assessment of drug targets. Theor Biol Med Model. 2006;3:27.
[36] Zhu XG, de Sturler E, Long SP. Optimizing the distribution of resources between enzymes of carbon metabolism can dramatically increase photosynthetic rate: a numerical simulation using an evolutionary algorithm. Plant Physiol. 2007;145:513–26.
[37] Xu S, Zhang X, Xu H, Dong B, Qu X, Chen B, et al. Silane modified upconversion nanoparticles with multifunctions: imaging, therapy and hypoxia detection. Sci Rep. 2016;6:22350.
[38] Kozuleva MA, Ivanov BN. Evaluation of the participation of ferredoxin in oxygen reduction in the photosynthetic electron transport chain of isolated pea thylakoids. Photosynth Res. 2010;105:51–61.
[39] Nikel PI, Zhu J, San KY, Mendez BS, Bennett GN. Metabolic flux analysis of Escherichia coli creB and arcA mutants reveals shared control of carbon catabolism under microaerobic growth conditions. J Bacteriol. 2009;191:5538–48.
[40] Chapman SP, Paget CM, Johnson GN, Schwartz JM. Flux balance analysis reveals acetate metabolism modulates cyclic electron flow and alternative glycolytic pathways in Chlamydomonas reinhardtii. Front Plant Sci. 2015;6:474.
[41] Boyle NR, Sengupta N, Morgan JA. Metabolic flux analysis of heterotrophic growth in Chlamydomonas reinhardtii. PLoS ONE. 2017;12:e0177292.
[42] Lauersen KJ, Baier T, Wichmann J, Wordenweber R, Mussgnug JH, Hubner W, et al. Efficient phototrophic production of a high-value sesquiterpenoid from the eukaryotic microalga Chlamydomonas reinhardtii. Metab Eng. 2016;38:331–43.
[43] Wichmann J, Baier T, Wentnagel E, Lauersen KJ, Kruse O. Tailored carbon partitioning for phototrophic production of (E)-α-bisabolene from the green microalga Chlamydomonas reinhardtii. Metab Eng. 2018;45:211–22.
[44] Venkanna D, Sudfeld C, Baier T, Homburg SV, Patel AV, Wobbe L, et al. Knock-down of the IFR1 protein perturbs the homeostasis of reactive electrophile species and boosts photosynthetic hydrogen production in chlamydomonas reinhardtii. Front Plant Sci. 2017;8:1347.
[45] Kasimova MR, Grigiene J, Krab K, Hagedorn PH, Flyvbjerg H, Andersen PE, et al. The free NADH concentration is kept constant in plant mitochondria under different metabolic conditions. Plant Cell. 2006;18:688–98.
[46] Igamberdiev AU, Gardeström P. Regulation of NAD-and NADP-dependent isocitrate dehydrogenases by reduction levels of pyridine nucleotides in mitochondria and cytosol of pea leaves. Biochim Biophys Acta Bioenerg. 2003;1606:117–25.
[47] London J, Knight M. Concentrations of nicotinamide nucleotide coenzymes in micro-organisms. Microbiology. 1966;44:241–54.
[48] Boyer PD, Lardy H, Myrbäck K, editor(s). The Enzymes. Vol. 3. USA: Academic Press; 1960.
[49] Takebe I, Kitahara K. Levels of nicotinamide nucleotide coenzymes in lactic acid bacteria. J Gen Appl Microbiol. 1963;9:31–40.
[50] Wimpenny JW, Firth A. Levels of nicotinamide adenine dinucleotide and reduced nicotinamide adenine dinucleotide in facultative bacteria and the effect of oxygen. J Bacteriol. 1972;111:24–32.
[51] Brody S. Regulation of pyridine nucleotide levels and ratios in Neurospora crassa. J Biol Chem. 1972;247:6013–7.

[52] Olin-Sandoval V, González-Chávez Z, Berzunza-Cruz M, Martínez I, Jasso-Chávez R, Becker I, et al. Drug target validation of the trypanothione pathway enzymes through metabolic modelling. FEBS J. 2012;279:1811–33.
[53] Ivarsson R, Quintens R, Dejonghe S, Tsukamoto K, Renström E, Schuit FC, et al. Redox control of exocytosis: regulatory role of NADPH, thioredoxin, and glutaredoxin. Diabetes. 2005;54:2132–42.
[54] Veech R, Eggleston L, Krebs H. The redox state of free nicotinamide–adenine dinucleotide phosphate in the cytoplasm of rat liver. Biochem J. 1969;115:609.
[55] Allue I, Gandelman O, Dementieva E, Ugarova N, Cobbold P. Evidence for rapid consumption of millimolar concentrations of cytoplasmic ATP during rigor-contracture of metabolically compromised single cardiomyocytes. Biochem J. 1996;319:463.
[56] Koop A, Cobbold PH. Continuous bioluminescent monitoring of cytoplasmic ATP in single isolated rat hepatocytes during metabolic poisoning. Biochem J. 1993;295:165.
[57] Bowers KC, Allshire AP, Cobbold PH. Bioluminescent measurement in single cardiomyocytes of sudden cytosolic ATP depletion coincident with rigor. J Mol Cell Cardiol. 1992;24:213–8.
[58] Ainscow EK, Rutter GA. Glucose-stimulated oscillations in free cytosolic ATP concentration imaged in single islet β-cells: evidence for a Ca2+-dependent mechanism. Diabetes. 2002;51:S162–70.
[59] Gribble FM, Loussouarn G, Tucker SJ, Zhao C, Nichols CG, Ashcroft FM. A novel method for measurement of submembrane ATP concentration. J Biol Chem. 2000;275:30046–9.
[60] Dennis PB, Jaeschke A, Saitoh M, Fowler B, Kozma SC, Thomas G. Mammalian TOR: a homeostatic ATP sensor. Science. 2001;294:1102–5.
[61] Miller D, Horowitz S. Intracellular compartmentalization of adenosine triphosphate. J Biol Chem. 1986;261:13911–5.
[62] Kennedy HJ, Pouli AE, Ainscow EK, Jouaville LS, Rizzuto R, Rutter GA. Glucose generates sub-plasma membrane ATP microdomains in single islet β-cells potential role for strategically located mitochondria. J Biol Chem. 1999;274:13281–91.

Supplementary Material: The online version of this article offers supplementary material (DOI: https://doi.org/10.1515/jib-2018-0018).